International Journal of Fluid Power, 2015
Vol. 16, No. 1, 11–24, http://dx.doi.org/10.1080/14399776.2015.1012437

Taylor & Francis
Taylor & Francis Group

Dimensioning of pneumatic cylinders for motion tasks

Matthias Doll[a]*, Rüdiger Neumann[a] and Oliver Sawodny[b]

[a]*Festo AG & Co. KG, Ruiterstr. 82, Esslingen, Germany;* [b]*Institute for System Dynamics, University of Stuttgart, Stuttgart, Germany*

(*Received 11 December 2014; accepted 23 January 2015*)

This paper proposes a novel method for dimensioning pneumatic cylinders for motion tasks. Considered are standard pneumatic cylinders with common directional control valves and exhaust flow throttles. The focus thereby is on the dimensioning of the cylinders for point-to-point motions regarding energy efficiency. The proposed strategy is based on the eigenfrequency and considers similarity transformations. The dimensioning of the cylinder diameter and the valve conductance bases upon a few algebraic equations leading to optimally sized pneumatic cylinders. Furthermore, the equations are used for classification purposes of the pneumatic cylinders regarding energy efficiency.

Keywords: pneumatic cylinders; dimensioning; energy efficiency; eigenfrequency

1. Introduction

Pneumatic cylinders are widely used as actuators for point-to-point (PTP) motions in industrial automation processes. They provide a high power density, low weight and low acquisition costs. Concerning energy efficiency, pneumatic cylinders are considered to be less efficient than electric drives. This shows that energy efficiency considerations of pneumatic cylinders are very important. The higher energy consumption of pneumatic drives is often caused by using oversized systems. Due to being open loop controlled, the consumption of compressed air depends on the pressure level and on the volume of the cylinder, indicating that the appropriate sizing plays an important role. Therefore, one main point regarding energy efficiency is the correct dimensioning of the cylinder.

For force-based applications, simple physical equations are used to dimension the cylinder (Bimba 2011). For motion-based applications, a simple way for determining the appropriate cylinder size is an outstanding topic which is addressed in this paper.

The state of the art of sizing pneumatic cylinders for motion tasks is very limited. Some publications are focused on the sizing of the tubing (Harvey 2003), filter and fittings (Kreher 2009) or valves (Foy 2003). The main approach is to reduce the pressure drops. The sizing of pneumatic drives is mainly focused on a damped system behaviour at stroke end with the aim to reduce the impact energy. All these considerations are indeed very important for dimensioning pneumatic cylinders. But the main aspect of sizing pneumatic cylinders concerning to a given PTP motion is not addressed yet. One main point regarding these missing dimensioning rules is the huge amount of possible applications, orientations but also the huge amount of mechanical restrictions and criteria, such that the aspect of energy efficiency is secondary. Furthermore, there are a lot of criteria concerning the dimensioning of drives (Malloy 2000, Danks 2008). Some criteria are:

- Fulfilment of the application (transition time, force at stroke end, etc.)
- velocity/energy at stroke end
- forces/workload of the guidance, lateral forces, etc.
- air consumption, energy demand.

These criteria restrict the range for determining an energy-efficient solution for pneumatic cylinders. A precise calculation formula for dimensioning the drives is missing. State of the art is a process of using the experience of engineers in combination with simulation tools (Hildebrandt 2009). Other approaches suggest computer-based expert systems (Dikici 2004) for a proper selection of the system components. The process of dimensioning is governed by gut instinct and rules of thumb, such as the workload (Asco 2005) of pneumatic cylinders. In a subsequent process, the determined components are validated by using simulation software.

This paper refers to the dimensioning process from a pneumatic point of view. Thus, additional restrictions such as the workload of the guidance are neglected.

1.1. Air consumption vs. dimensioning

Neglecting temperature effects, the air consumption of a pneumatic cylinder is determined by its volume V_c, the dead volume V_d of the tubing and the connections within the cylinder head, the supply pressure level p_s and the ambient pressure level p_0 to:

*Corresponding author. Email: doll@de.festo.com

$$V_0 = V_c \frac{p_s}{p_0} + V_d \frac{p_s - p_0}{p_0} \approx (V_c + V_d) \frac{p_s}{p_0}. \quad (1)$$

It depends solely on the component parameters, such as the volume and the pressure level. The load or the speed and transition time, respectively, have no influence on the amount of compressed air needed by the cylinder. This is a main difference to feedback-controlled drives, which only need as much energy as they need for the specified motion task.

Therefore, a motion task can be realised with several drives. This is shown in Figure 1 for two drives (with the following diameters: 25 and 50 mm). Both drives fulfil the same boundary condition concerning the transition time and transport the same mass. It shows that the characteristic of the dynamic behaviour depends on the cylinder size (see velocity). Besides this dynamical characteristic, the influence of system design concerning energy efficiency becomes evident. By means of the pneumatic force, it is visible that the force at stroke end is much higher than needed for the motion.

On the viewpoint of energy efficiency, mistakes are done very easily when dimensioning drives for motion tasks, thus the force at stroke end can be much higher than the force needed during motion. Besides a missing dimensioning formula, an objective criterion for evaluating existing systems is missing too. Without this evaluation criterion, energy efficiency strategies of different systems are hardly comparable. A method for classifying systems is proposed in this paper too.

The paper is structured as follows. In Section 2, the basic physical equations of the cylinder dynamics are presented. Section 3 treats a relative dimensioning approach. Thereby relative changes of some parameters are considered by using similarity considerations. These formulas are validated analytically in Section 4 using the differential equations of Section 2. The influence of all parameters is analysed. Section 5 then presents the dimensioning approach for pneumatic cylinders with pneumatic cushioning systems and suggests the approach for optimally sized cylinders. Furthermore, a possible classification scheme of pneumatic drives is proposed. Section 6 concludes this paper.

2. Modelling

The dynamics of a pneumatic cylinder is state of the art and refers to the modellation in Ohligschläger (1990). The main parts of the model are the mass flow equations, the pressure dynamics and the motion dynamics.

2.1. System set-up

The system considered in this paper is a standard controlled cylinder as shown in Figure 2. There are two types distinguished: rodless cylinders and cylinders with a rod. The control structure for both types is the same containing a 4/2-directional control valve and exhaust flow restrictors for an adjustment of the speed. The flow restrictors are only active for the exhaust flow.

2.2. Mass flow equations

The mass flows $\dot{m}_i, i \in \{a, b\}$ for both chambers 'a' and 'b' through the valve and the flow restrictors is described via the C-b-method (Bala 1985):

$$\dot{m}_i = C_i \rho_0 \psi(p_{ds}/p_{us}, b) p_{us}. \quad (2)$$

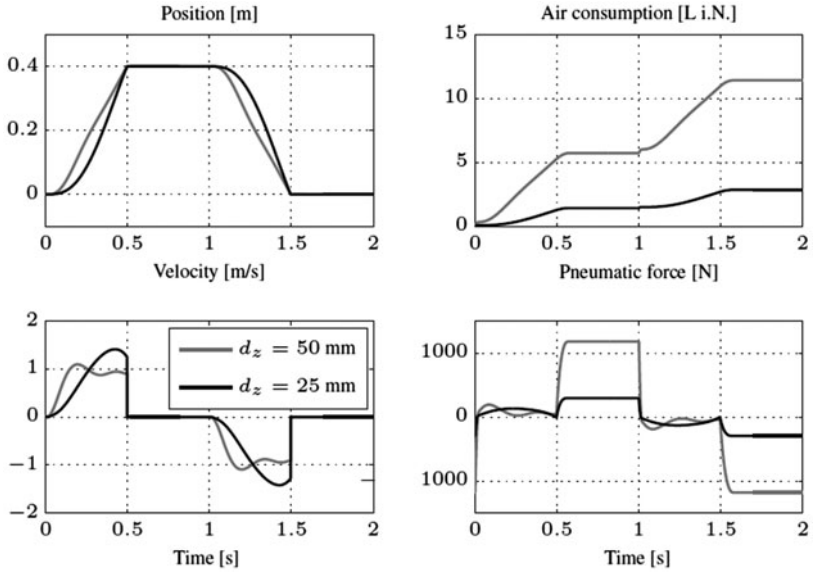

Figure 1. Comparison of the system dynamics and air consumption of two different cylinder sizes (*gray*: $d_c = 50$ mm, *black*: $d_c = 25$ mm) for the same application: load $m = 15$ kg, transition time $T_f = 0.5$ s, stroke length $l_c = 0.4$ m.

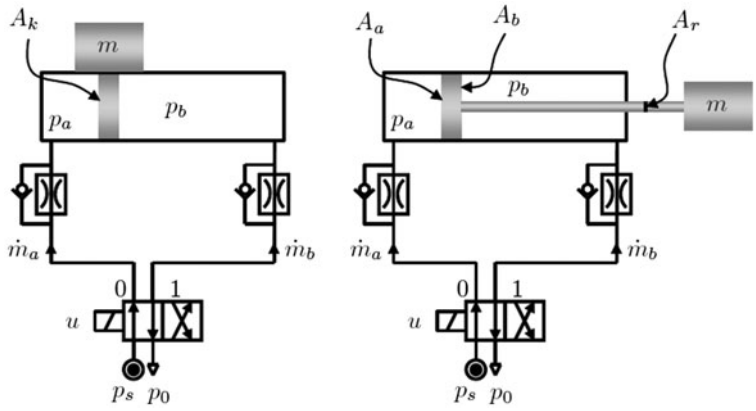

Figure 2. Pneumatic drive systems in standard configuration with exhaust flow throttles and a 4/2 directional control valve. *Left*: rodless cylinder, *right*: cylinder with a rod.

With C_i being the resulting sonic conductance, ρ_0 the density of air at standard conditions (ISO8778 2003), p_{us} the upstream pressure and p_{ds} the downstream pressure. The flow function $\psi(\cdot)$ is modelled as (Sanville 1971):

$$\psi\left(\frac{p_{ds}}{p_{us}}, b\right) = \begin{cases} 1, & q = \frac{p_{ds}}{p_{us}} < b, \\ \sqrt{1 - \left(\frac{\frac{p_{ds}}{p_{us}} - b}{1-b}\right)^2}, & q = \frac{p_{ds}}{p_{us}} \geq b, \end{cases} \tag{3}$$

distinguishing between choked ($q < b$) and unchoked ($q \geq b$) flow conditions. The exhaust flow throttles are considered as throttling factors $k_i \in [0, 1]$ which reduce the sonic conductance of the valve C_v:

$$C_i = C_v k_i, \quad \text{if } \dot{m}_i < 0, \quad i \in \{a, b\}. \tag{4}$$

Thus indicating that every flow path has its own value of the sonic conductance. For a general consideration, the mass flows for each flow path ij with $i \in \{a, b\}$ expressing the chamber and $j \in \{1, 2\}$ expressing the flow direction (1: venting, 2: exhausting) are expressed in dependency on u_{ij} which enables the corresponding flow paths:

$$\dot{m}_i = u_{ij} C_{ij} \rho_0 \psi(p_{ds}/p_{us}, b) p_{us}. \tag{5}$$

Thereby, the signals u_{ij} depend on the valve position $u \in \{0, 1\}$ of the switching valve:

$$\begin{array}{llll} u_{a1} = 1 - u, & C_{a1} = C_v, & \text{venting} \\ u_{a2} = u, & C_{a2} = C_v k_a, & \text{exhausting} \\ u_{b1} = u, & C_{b1} = C_v, & \text{venting} \\ u_{b2} = 1 - u, & C_{b2} = C_v k_b, & \text{exhausting} \end{array}. \tag{6}$$

Thus, the mass flows in the chamber i depend on the valve position u: $\dot{m}_i = \dot{m}_i(u)$.

2.3. Pressure dynamics

Considering the air as an ideal gas in combination with the assumption of a polytropic change of condition ($pv^n = const.$), the pressure dynamics of the chambers 'a' and 'b' is modelled as (Ohligschläger 1990):

$$\dot{p}_i = \frac{n}{V_i(x) + V_{di}} \left(R T_0 \dot{m}_i - p_i \dot{V}_i(\dot{x}) \right), \quad i \in \{a, b\}. \tag{7}$$

Being p_i the pressure of chamber i, x the position of the piston, $\dot{x}$ the velocity of the piston, n the polytropic index, R the gas constant of air, T_0 the temperature of air at standard conditions, $V_i(x)$ the volume and $\dot{V}_i(\dot{x})$ its gradient and V_{di} the dead volume of chamber i.

2.4. Motion dynamics

The equations of the motion dynamics are derived by applying Newton's law:

$$m\ddot{x} = F_p - F_g - F_{fr}(\dot{x}), \tag{8}$$

being m the load. The right-hand side consists out of three forces: the pneumatic force F_p, the gravity force F_g and the friction force F_{fr}. The pneumatic force is calculated by the pressures and the corresponding piston areas:

$$F_p = A_a p_a - A_b p_b - A_r p_0. \tag{9}$$

Being A_a the piston area for chamber 'a', A_b the piston area for chamber 'b', A_r the area of the rod and p_0 the ambient pressure. For dimensioning purposes, the areas A_b and A_r are assumed to be functions of the area A_a (Hildebrandt 2009). For cylinders with a rod, the following relation concerning the effective areas is determined:

$$\xi = \frac{A_b}{A_a} \approx 0.88, \quad \xi_r = 1 - \xi, \tag{10}$$

which is considered to be constant for different cylinder sizes and leads to the pneumatic force as:

$$F_p = A_a(p_a - \xi \quad p_b - \xi_r p_0). \tag{11}$$

For cylinders without a rod yields: $\xi = 1$ and $\xi_r = 0$, such that $A_k = A_a = A_b$. The gravity force is calculated in dependence on the mass m and the angle α:

$$F_g = mg \sin \alpha. \tag{12}$$

Finally, the friction force is assumed to be a combination of Coulomb and viscous friction:

$$F_{fr}(\dot{x}) = f_{cf} \text{ sign } (\dot{x}) + f_{vf}\dot{x}, \tag{13}$$

being $f_{cf,}$ the Coulomb friction coefficient and $f_{vf,}$ the coefficient for viscous friction.

2.5. Complete system

Using the definitions $x_1 = x$, $x_2 = \dot{x}$, $x_3 = p_a$, $x_4 = p_b$ of the states, the system is stated as:

$$\dot{x}_1 = x_2, \tag{14a}$$

$$\dot{x}_2 = \frac{1}{m}\left(A_a(x_3 - \xi x_4 - \xi_r p_0) - mg \sin \alpha - F_{fr}(x_2)\right), \tag{14b}$$

$$\dot{x}_3 = \frac{n}{V_a(x_1) + V_{da}}(RT_0\dot{m}_a(u) - x_3 A_a x_2), \tag{14c}$$

$$\dot{x}_4 = \frac{n}{V_b(x_1) + V_{db}}(RT_0\dot{m}_b(u) + x_4 A_b x_2). \tag{14d}$$

Using the state vector $x = [x_1, x_2 x_3, x_4]$ and the input u, the system equations are stated as follows:

$$\Sigma: \quad \dot{\boldsymbol{x}}(t) = \boldsymbol{f}(\boldsymbol{x}(t), u(t)). \tag{15}$$

2.6. Energy consumption

The energy consumption of a pneumatic drive is calculated by the air consumption and the rating number of compressed air (Weiß 2008). This rating number expresses the amount of electric energy W_{cp} needed by the compressor to build up the consumed compressed air. The consumed air is calculated by the integral over the supplied mass flow $\dot{m}_s = \dot{\tilde{m}}_a + \dot{\tilde{m}}_b$, with $\dot{\tilde{m}}_i = \dot{m}_i \cdot (\dot{m}_i > 0)$ and is transformed to standard litres via the density of air at standard conditions ρ_0:

$$V_0 = \frac{1}{\rho_0}\int_{t_0}^{t} \dot{m}_s d\tau. \tag{16}$$

Due to the linear relationship between V_0 and W_{cp}, energy efficiency considerations are equivalent for both: reducing V_0 and reducing W_{cp}. In standard pneumatic control mode, the chambers are always filled up to the supply pressure level p_s. Therefore, the air consumption can be easily determined using (1). In combination with the definition $L = l_c + l_d$ and $V_c + V_d = A_k L$ yields for a rodless cylinder:

$$V_0 = A_k L \frac{p_s}{p_0}. \tag{17}$$

3. Relative dimensioning

In this section, the system behaviour is analysed when individual parameters are changed. The aim is to preserve the system behaviour when parameter variations are considered, such that with an appropriate dimensioning of the system components, the influence of the parameter variations on the system dynamics is compensated. This is done by similarity considerations.

3.1. Problem formulation

A PTP motion is described by mainly four parameters: the moved mass m, the stroke length l_c, the transition time T_f and the pressure level p_s:

$$\mathcal{A} = \{m, l_c, T_f, p_s\}. \tag{18}$$

The system is mainly described by two parameters: the cylinder diameter d_c and the sonic conductance of the valve C_v:

$$\mathcal{S} = \{d_c, C_v\}. \tag{19}$$

The stroke length of the cylinder is considered to match the required stroke length of the PTP motion l_c because motions between both end points of the cylinder are considered. The process of system dimensioning is described by a relation between the system parameters $\mathcal{S}$ and the application parameters $\mathcal{A}$, such that the specified application is fulfilled with the selected system. Thereby two dimensioning approaches are considered:

- relative dimensioning
- absolute dimensioning

The aim of the relative dimensioning is to find out characteristic equations reflecting the relations between system and application parameters. This is done by similarity considerations between two systems and is the objective of the current section. The aim of the absolute dimensioning is to find a function which relates directly the system parameters to the application parameters without the detour of considering a reference system. This absolute dimensioning is treated in Section 5.

3.2. Cylinder eigenfrequency

The pneumatic cylinder is considered as a mass m, which is connected to a spring. The system stiffness is a result of the compressibility of air. For determining the stiffness, the chambers are considered to be closed, such that the mass of compressed air is kept constant in both chambers. The stiffness c of the spring is defined by the stiffness of the system using the pneumatic force (9):

$$c(x) = \left|\frac{\partial F}{\partial x}\right| = A_a p\left(\frac{1}{x + l_{da}} + \frac{\xi}{l_c - x + l_{db}}\right), \tag{20}$$

being p the pressure level of the chambers and x the piston position. Due to the system nonlinearities, the stiffness depends on the actual position x. Figure 3 shows the stiffness for a rodless actuator (with $\xi = 1$) in dependence on the initial position x and the pressure level p. The minimum stiffness is achieved in the middle position. The eigenfrequency ω_0 of pneumatic cylinders is formally determined by the stiffness c (20) and the well-known relation $\omega_0 = \sqrt{c/m}$ (Eschmann 1994). For ease of calculation, the following assumptions are drawn:

- A rodless cylinder is considered: $\xi = 1$.
- The dead volumes are considered to be equal: $l_{da} = l_{db} = l_d$.
- The eigenfrequency is determined in the middle position $x = l_c/2$ (Scholz 1990) leading to the minimal eigenfrequency.

These assumptions are proved later on. The eigenfrequency is determined by:

$$\omega_0 = \frac{2\pi}{T^0} = \sqrt{\frac{4A_k^2 p}{m(V_c + V_d)}}. \tag{21}$$

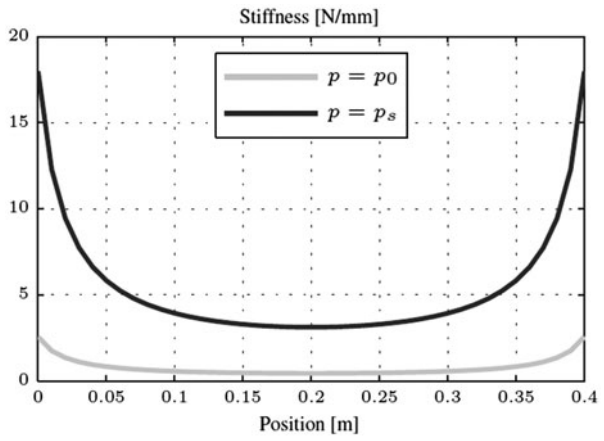

Figure 3. Stiffness of a pneumatic, rodless actuator with $d_c = 25$ mm, $l_c = 400$ mm and $l_d = l_{da} = l_{db} = 2$ cm in dependence on the position and the pressure level.

With T^0 as the period of the oscillation at eigenfrequency. Both chambers are closed and contain compressed air at a pressure level of p. With $V_c + V_d = A_k(l_c + 2l_d)$ and $l_c + 2l_d := L$, the eigenfrequency becomes:

$$\omega_0 = \frac{2\pi}{T^0} = \sqrt{\frac{4A_k p}{mL}}. \tag{22}$$

It is the frequency of oscillation and thus expresses the speed of the piston. It is a characteristic number and is often used for servo pneumatic controller design (Göttert 2003, Hildebrandt 2009). Because of influencing the bandwidth of the controller, the eigenfrequency is determined in the mid position reflecting the minimum eigenfrequency, and thus the minimum bandwidth. In this paper, the eigenfrequency is used for dimensioning purposes for PTP motions. The eigenfrequency is considered to be a characteristic number reflecting the system dynamics. The idea for the dimensioning approach is to keep the eigenfrequency constant – independent on variations of the mass, the stroke length or the pressure level. Equation (22) reflects the characteristic relations between the system and application parameters and thus provides answers concerning the influence of variations of individual parameters on the piston area. For example, when the mass is doubled, according to (22), a doubled piston area is needed to achieve the same eigenfrequency.

Equation (22) contains almost all parameters of the application parameters $\mathcal{A}$ in (18) and the system parameters $\mathcal{S}$ in (19). Two parameters are missing: the transition time T_f and the sonic conductance C_v. The determination of the characteristic equations including these parameters is addressed in the next sections.

3.3. Pneumatic frequency ratio

In this section, a new characteristic number is introduced which includes the transition time T_f. Hence, a relation for the speed of the piston is needed. The speed of an oscillation is implicitly given by the eigenfrequency: $T^0 = 2\pi/\omega_0$. A high eigenfrequency thus means that a small period T^0 is achieved and indicates that a small transition time T_f can be reached. Therefore, a proportional dependency between the possible transition time T_f and the period T^0 is used: $T_f = \Omega \cdot T^0$. It indicates that if a low velocity or a high transition time T_f is requested, a low eigenfrequency ω_0 is necessary. This leads to the definition of the pneumatic frequency ratio (PFR):

$$\Omega = \frac{\omega_0}{\omega_f} = \frac{T_f}{T^0} \tag{23}$$

It describes the ratio of the eigenfrequency ω_0 and the frequency $\omega_f = 2\pi/T_f$ which is given by the transition time T_f. In combination with (22), a characteristic

equation for the cylinder size containing all relevant parameters including the transition time T_f is obtained:

$$\Omega = \omega_0 \frac{T_f}{2\pi} = \frac{T_f}{\pi} \sqrt{\frac{A_k p}{mL}}. \tag{24}$$

Thereby, the parameters T_f, p, m and L are termed characteristic quantities.

As before, a double mass is compensated by a double piston area. But now, it's possible to answer the question on how to adjust the piston area if the transition time is halved: the piston area has to be increased by a factor of four.

3.4. Characteristic equation for the piston area

Using Equation (24), a characteristic equation for determining the cylinder size is obtained:

$$A_k = \pi^2 \Omega^2 \frac{mL}{T_f^2 p_s} = K_A \frac{mL}{T_f^2 p_s}. \tag{25}$$

Thereby the PFR Ω has to be given and K_A is constant.

3.5. Characteristic equation for the sonic conductance

For the determination of the valve size (namely the sonic conductance C_v), a mean value of the mass flow is used. It is calculated by using (17):

$$\bar{\dot{m}} = \frac{\rho_0 V_0}{T_f} = \rho_0 A_k L \frac{p_s}{p_0} \frac{1}{T_f}. \tag{26}$$

In combination with the mass flow (2) of the venting chamber, an equation for the sonic conductance C_a is obtained:

$$C_a = \frac{1}{p_0 \psi(p_a/p_s, b)} \frac{A_k L}{T_f}. \tag{27}$$

Using (25) yields:

$$C_a = \frac{\pi^2 \Omega^2}{p_0 \psi(p_a/p_s, b)} \frac{mL^2}{T_f^3 p_s} = K_{Ca} \frac{mL^2}{T_f^3 p_s}. \tag{28}$$

Thereby the flow function $\psi(p_a/p_s, b)$ is assumed to be invariant because of obtaining invariant pressure trajectories when using the proposed dimensioning approach. This will be proved in Section 4. The same approach for the exhausted chamber 'b' yields an equation for the sonic conductance C_b:

$$C_b = \frac{p_s}{p_0 \psi(p_0/p_b, b) p_b} \frac{A_k L}{T_f}. \tag{29}$$

The pressure p_b is considered to be dependent on the chosen supply pressure level: $p_b(t) = K(t) p_s$, with $K(t)$ being an invariant scaling factor. Additionally, $\psi(p_0/p_b, b)$ is assumed to be invariant as for the venting chamber. With (25) yields for the sonic conductance of the exhausted chamber:

$$C_b = \frac{\pi^2 \Omega^2}{p_0 \psi(p_0/p_b, b) K(t)} \frac{mL^2}{T_f^3 p_s} = K_{Cb} \frac{mL^2}{T_f^3 p_s}. \tag{30}$$

It shows the same proportional relation as (28) but with a different proportional constant K_{Cb}, leading to the following characteristic equation of the sonic conductance:

$$C_v = K_C \frac{mL^2}{T_f^3 p_s} \tag{31}$$

which is equal for both chambers 'a' and 'b'. The factor K_C depends on the flow function $\psi(p/p_s, b)$. Thus, for the venting chamber, it is calculated as:

$$K_{Ca} = \frac{\pi^2 \Omega^2}{p_0 \psi(p_a/p_s, b)}. \tag{32}$$

For the exhaust chamber yields:

$$K_{Cb} = \frac{\pi^2 \Omega^2}{p_0 \psi(p_b/p_0, b) K(t)}. \tag{33}$$

Using these equations, the sonic conductance depends on the piston area A_k (see Equations (27) and (29)) and thus the dimensioning approach is split up into two steps:

(1) Selecting a proper cylinder diameter by using (25).
(2) Selecting the correct valve according to (31).

Equations (25) and (31) depend both on the PFR Ω. Equation (31) for the sonic conductance additionally depends on the flow function $\psi(\cdot)$. These unknown parameters, however, are important for using the dimensioning functions. The determination of these proportional factors is part of Section 5.

3.6. Relative dimensioning

In this section, both Equations (25) and (31) are used for a relative dimensioning of the system components. Thereby *relative dimensioning* refers to a relative consideration of two systems. The system dynamics of system Σ^r with the application parameters m^r, L^r, T_f^r, p_s^r and the system parameters A_k^r, C_v^r should be transferred to system Σ, with the application parameters m, L, T_f, p_s and the system parameters A_k, C_v. According to (25) and (31), the system parameters have to be scaled as follows:

$$\begin{aligned}\frac{A_k}{A_k^r} &= \left(\frac{T_f^r}{T_f}\right)^2 \frac{mLp_s^r}{m^r L^r p_s} =: \zeta_A.\\ \frac{C_v}{C_v^r} &= \frac{m}{m^r}\left(\frac{T_f^r}{T_f}\right)^3 \left(\frac{L}{L^r}\right)^2 \frac{p_s^r}{p_s} =: \zeta_C.\end{aligned} \tag{34}$$

Being ζ_A, the scaling factor for the piston area: $A_k = \zeta_A A_k^r$ and ζ_C, the scaling factor for the sonic conductance of the valve: $C_v = \zeta_C C_v^r$.

Remark: The scaling functions (34) are determined on the basis of the PFR (23). As shown in Figure 3, the eigenfrequency depends on both the position and the pressure level. This, however, does not restrict the approach of using the eigenfrequency which is determined in the middle position. Because of comparing two systems, the ratio between both eigenfrequencies is the same, independent of the position used for calculating the eigenfrequency. This and other assumptions made in this section concerning invariant trajectories will be proved analytically in Section 4.

4. Validation

In this section, the scaling functions (34) will be proved analytically using the system equations (14). Thereby, one has to keep in mind that if the stroke length is varied: $l_c = k \cdot l_c^r$, but the transition time is kept constant $T_f = T_f^r$, the velocity trajectory of the piston has to fulfil the following relation:

$$x_2(t) = \frac{l_c}{l_c^r} x_2^r(t), \tag{35}$$

such that the system dynamics of system Σ is similar to the reference system Σ^r. Comparable relations are obtained when considering variations of the transition time T_f or the pressure level p_s. For a proper consideration of all parameter variations, the trajectories will be normalised in time:

$$\tau = \frac{1}{T_f} t \in [0,1], \quad \mathrm{d}\tau = \frac{1}{T_f}\mathrm{d}t, \tag{36}$$

being τ the normalised time. Furthermore, the state trajectories are also normalised in their values:

$$\begin{aligned}\tilde{\boldsymbol{x}}(\tau) &= \boldsymbol{D}(\boldsymbol{p}) \cdot \boldsymbol{x}(t),\\ \boldsymbol{D}(\boldsymbol{p}) &= \mathrm{diag}\left\{\left[\tfrac{1}{l_c}, \quad \tfrac{T_f}{l_c}, \quad \tfrac{1}{p_s}, \quad \tfrac{1}{p_s}\right]\right\}\end{aligned} \tag{37}$$

being $\tilde{\boldsymbol{x}}$ the normalised states and $\boldsymbol{D}(\boldsymbol{p})$ a parameter-dependent scaling matrix with $\boldsymbol{p} = \left[l_c, T_f, p_s\right]$. Trajectories of two systems Σ and Σ^r are considered to be similar if their trajectories in normalised coordinates match:

$$\tilde{\boldsymbol{x}}(\tau) = \tilde{\boldsymbol{x}}^r(t^r). \tag{38}$$

This leads to the following condition on the states:

$$\boldsymbol{x}(t) = \mathrm{diag}\left\{\left[\tfrac{l_c}{l_c^r}, \quad \tfrac{T_f^r l_c}{T_f l_c^r}, \quad \tfrac{p_s}{p_s^r}, \quad \tfrac{p_s}{p_s^r}\right]\right\}\boldsymbol{x}^r(t^r). \tag{39}$$

Figure 4 illustrates what is meant with similarity of trajectories. Two systems Σ and Σ^r with different diameters d_c and d_c^r achieve different transition times T_f and T_f^r, but due to the scaling function (39), the velocity profile of system Σ is scaled and matches the velocity profile of system Σ^r. This indicates that both systems are similar. Using (39) in combination with (36), the following dynamical condition on the states is achieved:

$$\dot{\boldsymbol{x}}(t) = \left(\frac{T_f^r}{T_f}\right)\mathrm{diag}\left\{\left[\tfrac{l_c}{l_c^r}, \quad \tfrac{T_f^r l_c}{T_f l_c^r}, \quad \tfrac{p_s}{p_s^r}, \quad \tfrac{p_s}{p_s^r}\right]\right\}\dot{\boldsymbol{x}}^r(t^r). \tag{40}$$

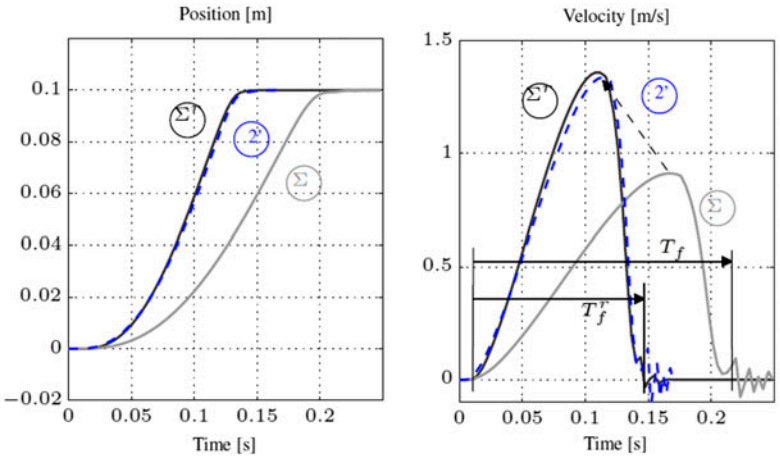

Figure 4. Illustration of a similar system dynamics between two systems (*black*: reference system Σ^r with $d_c^r = 20$ mm and $T_f^r = 0.125$ s, *gray*: system Σ with $d_c = 32$ mm and $T_f = 0.2$ s). Both are parameterised equally with: $m = 10$ kg and $l_c = 0.1$ m. The scaled trajectories of system Σ (*blue*) are similar to the trajectories of the reference system Σ^r.

For analysation purposes, the validation of the system dynamics is split up into two parts considering the motion dynamics and the pressure dynamics to be independent.

4.1. Analysis of the motion dynamics

For the analysation of the motion dynamics, the scalings (34) for the piston area and the sonic conductance are used together with the normalisation of the states (37) in the differential equations for the position (14a) and the velocity (14b). Thereby the differential equation for the position is related purely by a kinematic relationship with the velocity, such that the error dynamics $\dot{e}_1 = \dot{x}_1^r - \frac{T_f l_c^r}{T_f^r l_c}\dot{x}_1 = 0$ disappears. For the dynamics of the velocity (14b) yields:

$$\begin{aligned}\dot{x}_2 &= \frac{1}{m}\left(A_a.(x_3 - \xi x_4 - \xi_r p_0) - F_{fr}(x_2)\right) - g\sin\alpha = \frac{1}{m}\left[\left(\frac{T_f^r}{T_f}\right)^2 \frac{m}{m^r}\frac{l_c}{l_c^r}\frac{p_s^r}{p_s}A_a^r \cdot \left(\frac{p_s}{p_s^r}x_3^r - \xi\frac{p_s}{p_s^r}x_4^r - \xi_r p_0\right) - F_{fr}(x_2)\right] - g\sin\alpha \\ &= \left(\frac{T_f^r}{T_f}\right)^2 \frac{l_c}{l_c^r}\frac{1}{m^r}\left[A_a^r \cdot \left(x_3^r - \xi x_4^r - \xi_r\frac{p_s^r}{p_s}p_0\right) - \frac{m^r}{m}\left(\frac{T_f}{T_f^r}\right)^2 \frac{l_c^r}{l_c}F_{fr}(x_2)\right] - g\sin\alpha.\end{aligned} \tag{41}$$

The error dynamics $\dot{e}_2 = \dot{x}_2^r - \left(\frac{T_f}{T_f^r}\right)^2 \frac{l_c^r}{l_c}\dot{x}_2 = 0$ between both the systems leads to:

$$\begin{aligned}\dot{e}_2 = &\underbrace{-\frac{A_a^r}{m^r}\xi_r\left(1 - \frac{p_s^r}{p_s}\right)p_0}_{I} \\ &\underbrace{-\frac{1}{m^r}\left(F_{fr}^r(x_2^r) - \frac{m^r}{m}\left(\frac{T_f}{T_f^r}\right)^2 \frac{l_c^r}{l_c}F_{fr}(x_2)\right)}_{II} \\ &\underbrace{-\left(1 - \left(\frac{T_f}{T_f^r}\right)^2 \frac{l_c^r}{l_c}\right)g\sin\alpha}_{III},\end{aligned} \tag{42}$$

which has to disappear, such that invariant trajectories are obtained: $\dot{e}_2 = 0$. According to (42), three conditions have to be fulfilled. The first condition (I) disappears if the supply pressure is kept constant $p_s = p_s^r$ or if a rodless cylinder is used: $\xi_r = 0$. The second condition (II) is a condition for the friction force to gain invariant trajectories. For a detailed analysis, the Coulomb friction f_{cf} and the viscous friction f_{vf} have to be considered separately resulting in the following relations:

$$\begin{aligned}f_{cf} &= f_{cf}^r \frac{m}{m^r}\left(\frac{T_f^r}{T_f}\right)^2 \frac{l_c}{l_c^r} = \zeta_A \cdot f_{cf} \cdot \frac{p_s}{p_s^r}, \\ f_{vf} &= f_{vf}^r \frac{m}{m^r}\frac{T_f^r}{T_f}.\end{aligned} \tag{43}$$

This shows that the Coulomb friction has to grow proportionally with the piston area. But with one restriction: if the supply pressure is varied, the piston area is adjusted by (34), such that the same pneumatic force is achieved. The friction has to be proportional to the pneumatic force, such that it has to be independent on the pressure level.

The viscous friction depends on the velocity, such that the relations for the corresponding coefficient f_{vf} are slightly different: it has to be independent of the stroke length and has to grow linearly with the diameter when the transition time is varied.

Both the viscous friction coefficient and the coulomb friction coefficient typically grow linearly with the diameter because of being dependent on the circumference of the piston. Therefore, the necessary dependencies in (43) on the friction typically are not fulfilled. This will be analysed later on.

The third condition (III) of Equation (42) is a condition on the gravity force which should be varied in dependence on the transition time or the stroke length. But the gravity force cannot be varied, such that the error dynamics does not disappear and the result is falsified.

4.2. Analysis of the pressure dynamics

The analysis of the pressure dynamics is performed analogue to the analysis of the motion dynamics. Without loss of generality (w.l.o.g.), chamber 'a' is assumed to be vented and chamber 'b' is assumed to be exhausted. A further assumption refers to the length of the dead volume: l_d, which is assumed to be proportional to the stroke length $l_d = l_c/l_c^r \cdot l_d^r$. Using the abbreviation: $x_{1a} = x_1 + l_{da}$, for chamber 'a' yields:

$$\begin{aligned}\dot{x}_3 &= \frac{n}{A_a x_{1a}}\left[RT_0 C_a \rho_0 \psi\left(\frac{x_3}{p_s}, b\right)p_s - A_a x_3 x_2\right] \\ &= \frac{T_f^r}{T_f}\frac{p_s}{p_s^r}\underbrace{\frac{n}{A_a^r x_{1a}^r}\left[RT_0 C_a^r \rho_0 \psi\left(\frac{x_3^r}{p_s}, b\right)p_s^r - A_a^r x_3^r x_2^r\right]}_{=\dot{x}_3^r} \\ &= \frac{T_f^r}{T_f}\frac{p_s}{p_s^r}\dot{x}_3^r\end{aligned} \tag{44}$$

an unrestricted, invariant system dynamics because of the disappearance of the error dynamics $\dot{e}_3 = \dot{x}_3^r - \frac{T_f}{T_f^r}\frac{p_s^r}{p_s}\dot{x}_3 = 0$. Using the abbreviation for chamber 'b': $x_{1b} = l_c - x_1 + l_{db}$ yields:

$$\begin{aligned}\dot{x}_4 &= \frac{n}{A_b x_{1b}}\left[RT_0 C_b \rho_0 \psi\left(\frac{p_0}{x_4}, b\right)x_4 + A_b x_4 x_2\right] \\ &= \frac{T_f^r}{T_f}\frac{p_s}{p_s^r}\underbrace{\frac{n}{A_b^r x_{1b}^r}\left[RT_0 C_b^r \rho_0 \psi\left(\frac{p_0}{x_4^r}\frac{p_s^r}{p_s}, b\right)x_4^r + A_b^r x_4^r x_2^r\right]}_{\stackrel{!}{=}\dot{x}_4^r},\end{aligned} \tag{45}$$

with the error dynamics $\dot{e}_4 = \dot{x}_4^r - \frac{T_f}{T_f^r}\frac{p_s^r}{p_s}\dot{x}_4 = 0$:

$$\dot{e}_4 = \frac{nRT_0 C_v^r}{A_b^r x_{1b}^r}\left[\psi\left(\frac{p_0}{x_4^r}, b\right) - \psi\left(\frac{p_0}{x_4^r}\frac{p_s^r}{p_s}, b\right)\right]x_4^r, \tag{46}$$

which disappears with the following condition on the flow function:

$$\psi\left(\frac{p_0}{x_4^r}\frac{p_s^r}{p_s}, b\right) = \psi\left(\frac{p_0}{x_4^r}, b\right). \tag{47}$$

This condition is fulfilled if the supply pressure is kept constant: $p_s = p_s^r$, such that an invariant system dynamics is obtained. If a variation of the supply pressure is considered, condition (47) holds only for choked flow conditions with $\psi = 1$ (see Equation (3)) and leads to a condition on the pressures (the b value is considered to be constant): $p_0/x_4 < b$ and $p_0 p_s^r/(x_4^r p_s) < b$.

All necessary conditions for an invariant system dynamics are listed in Table 1. Most restrictions exist for the variation of the supply pressure. All other parameter variations are influenced by a mismatching friction force. Therefore, an exact, transferability of the system dynamics is not reached. In the light of being much lower than the cylinder force, the influence of the mismatching friction force however is inferior.

5. Dimensioning of pneumatic systems

In Section 4, it has been illustrated that the scaling functions (34) indeed lead to invariant system dynamics (under certain conditions given in Table 1). Thereby, the scaling functions (34) are derived using (25) and (31) and keeping Ω constant. This leads to the absolute dimensioning function, which is directly used for dimensioning cylinders and valves in dependence on the given application $\mathcal{A}$ and Ω, such that Ω is considered as a design factor and has to be well chosen. This is part of the following section.

5.1. Determination of optimal PFR

One main quantity in the dimensioning process is the impact energy at stroke end. A too high kinetic energy reduces the lifetime of the cylinder. Therefore, the kinetic energy at stroke end has to be reduced. This can be done by hydraulic shock absorbers, but is typically done by pneumatic cushioning systems. These cushioning systems are adjusted by a variable throttle. This throttle influences the dynamic behaviour at stroke end and thus has to be adjusted well, such that it absorbs the whole kinetic energy.

A pneumatic system which fulfils the restriction of the maximum impact energy at stroke end is considered to be a realisable system. Such a realisable system is called an optimal system if there exists no smaller cylinder which is realisable. Thus, an optimal system needs the minimum of compressed air. In this section, the PFR is determined for optimal systems.

This is done by simulations using CACOS[1] (Computer Aided Cylinder Optimisation System) – a simulation tool of Festo AG & Co. KG. CACOS is based upon the equations shown in Section 2. The simulation results match quite well the real pneumatic behaviour.

For a given system, CACOS varies both: the exhaust flow throttle and the cushioning throttle. It delivers the minimum transition time which is possible under the restriction of a damped system behaviour taking the

Table 1. Necessary conditions on the motion and pressure dynamics for an invariant system dynamics using the scaling functions (34).

	Motion dynamics				Pressure dynamics	
Parameter variation	Friction	Order	Rodless needed?	Compensation of gravity force?	Vented chamber	Exhausted chamber
m	$f_{cf} = f_{cf}^r\left(d_c/d_c^r\right)^2$ $f_{vf} = f_{vf}^r\left(d_c/d_c^r\right)^2$	2 2	No	Yes	–	–
T_f	$f_{cf} = f_{cf}^r\left(d_c/d_c^r\right)^2$ $f_{vf} = f_{vf}^r\left(d_c/d_c^r\right)$	2 1	No	No	–	–
L	$f_{cf} = f_{cf}^r\left(d_c/d_c^r\right)^2$ $f_{vf} = f_{vf}^r$	2 0	No	No	–	–
p_s	$f_{cf} = f_{cf}^r$ $f_{vf} = f_{vf}^r$	0 0	Yes	Yes	–	$q = p_0/x_4 < b$ Choked flow conditions

kinetic energy into account. Simulative studies were done for more than 750 systems with a huge range of parameters:

$d_c = 16\,\text{mm}...63\,\text{mm}$, $l_c = 50\,\text{mm}...1000\,\text{mm}$, $m = 1\,\text{kg}...38\,\text{kg}$. The resulting transition times are in the range $T_f = 50\,\text{ms}...2000\,\text{ms}$. Figure 5 shows the distribution of the simulations over the PFR for a stroke length of $l_c = 250\,\text{mm}$.

It is visible that an optimal PFR is achieved in the range of $\Omega \in [1, 2]$. Figure 5 shows also an accumulation of the simulations at $\Omega = 1$. According to (24), this implies that the eigenfrequency ω_0 matches the frequency ω_f, which is given by the transition time T_f and shows that an optimal cylinder selection is given when the system is operated in eigenfrequency mode.

For each parameter combination, the PFR is computed according to (24) and plotted against the diameter and the stroke length in Figure 6.

The size of the circles reflects the number of simulations according to Figure 5. Again a range of $\Omega \in [1, 2]$ with an accumulation at $\Omega = 1$ is visible.

Thereby the simulative approach of finding the minimum transition time (for a given system) for which a damped system behaviour is achieved is equivalent to an energy optimal cylinder selection. When an energy optimal cylinder is searched for a required transition time T_f, the cylinder has to be the minimal one (according to (1)), which fulfils the specified application. In turn, the selected cylinder reaches the minimum transition time and thus shows that the given approach above delivers an energy-efficient selection of the cylinder.

Figure 6 shows a dependency of the PFR on the stroke length, where low PFRs are achieved only for strokes between 100 and 500 mm. For long strokes >500 mm, the PFR increases, too. This is a result of the pneumatic cushioning system whose damping length l_{damp} does not depend on the stroke length, but only on the diameter of the cylinder. The relative damping length $l_{damp}^{rel} = l_{damp}/l_c$ therefore decreases with the stroke length expressing that the kinetic energy has to be absorbed on a shorter length. This is an unbalance for similarity considerations and thus an increased PFR is needed to achieve damped system behaviour.

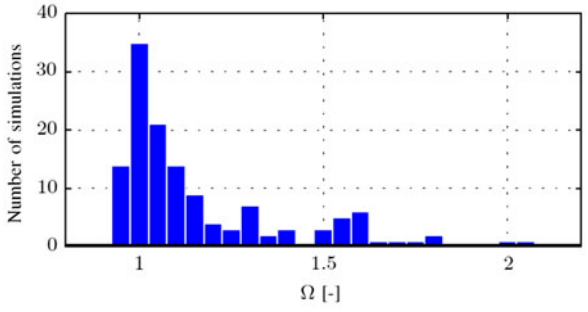

Figure 5. Histogram of PFR distribution of the simulation results for $l_c = 250$ mm.

The variations of Ω in Figure 6 are mainly a result of a mismatching friction force according to Table 1. But also the assumption of a proportional dead volume length $l_{di} \propto l_c$ has an influence on the residual errors.

The resulting system dynamics by means of the velocity are shown in Figure 7 for several systems with $\Omega = 0.98$. It illustrates that the resulting velocity profiles are similar to each other. Furthermore, it shows that the velocity profiles possess one sole oscillation/wave and shows that the eigenfrequency ω_0 of the system is matched.

5.2. *Determination of the minimal sonic conductance*

Besides the cylinder, the sonic conductance C_v of the valve is determined by using (31). The mean value of the flow function $\psi(p_a/p_s, b)$ for one stroke is measured on basis of the simulation data for the venting chamber. It is determined to: $\psi(p_a/p_s, b) \approx 0.4$. With it, a factor K_C is calculated according to (32): $K_{Ca} = 0.25 \cdot 10^3$. With those constants, the sonic conductance of the valve is dimensioned.

The exhaust flow throttles are considered as throttling factors reducing the sonic conductance of the valve. Therefore, their influence on the system dynamics is stronger than the sonic conductance of the valve, such that larger valves with greater C values can be used for the same application.

5.3. *Classification of pneumatic drive systems*

As shown in the preceding section, the achieved system dynamics is specified by the PFR. This shows that the PFR is a characteristic factor of the system dynamics. The system dynamics for several different PFRs is shown in Figure 8 by means of the profile of normalised velocity and normalised pressure. Thereby the pneumatic cushioning system is neglected, resulting in slightly different velocity profiles for $\Omega = 1$ in comparison to Figure 7.

Figure 8 shows that the count of oscillations in the velocity profile is directly related to the PFR. Therefore, the PFR can be read out of the velocity profile and is useful for the evaluation of systems. It shows that the PFR is a characteristic factor of the system dynamics and thus is used for a classification of systems. A possible classification including safety factors is shown in Table 2.

The dimensioning approach is useful also for other objectives than energy efficiency. E.g. for applications where a constant velocity is needed, a PFR of $\Omega > 2$ instead of $\Omega = 1$ should be selected. Concerning energy efficiency, the PFR expresses the factor with which the cylinder diameter d_c can be reduced:

$$d_c^* = \frac{d_c}{\Omega}, \tag{48}$$

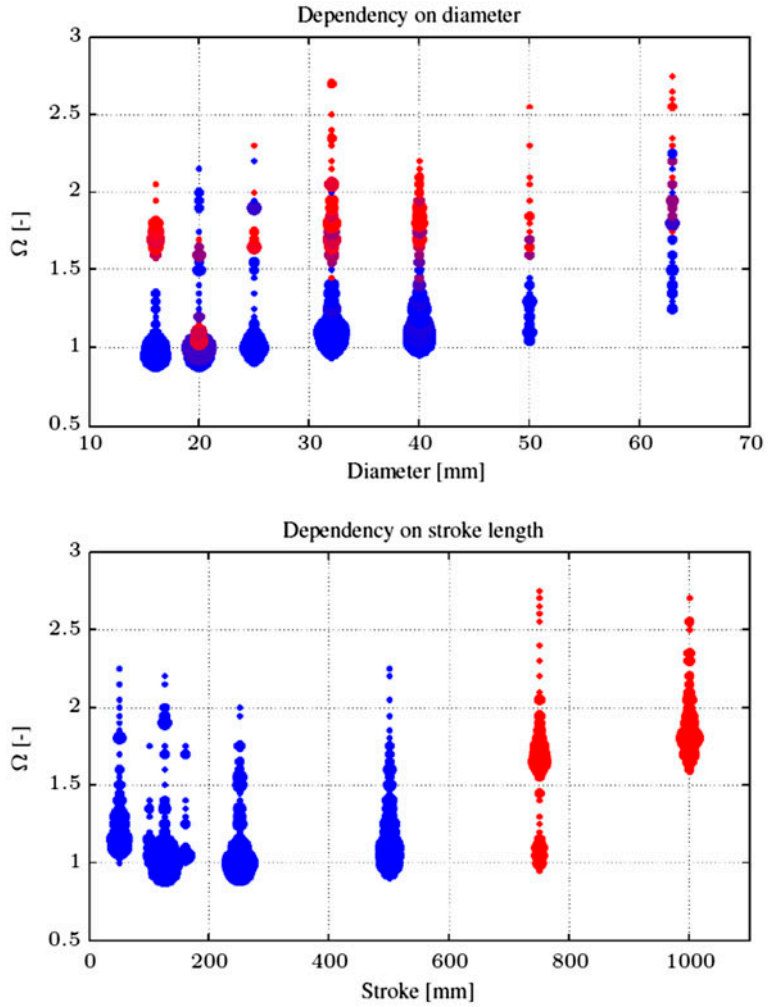

Figure 6. Scattered plot of the PFR of the validation data. The size of the blue circles is proportional to the amount of matching data points. *Top*: Dependency of Ω on the diameter, *bottom*: Dependency of Ω on the stroke. The red points refer to a stroke length above 600 mm.

where d_c^* is the optimal cylinder diameter leading to the optimal PFR of $\Omega^* = 1$. Thus, the PFR expresses the possibility to reduce the cylinder size.

According to (25), the PFR expresses also the possibility to reduce the transition time T_f:

$$T_f^* = \frac{T_f}{\Omega}, \tag{49}$$

where again the optimal transition time is denoted by T_f^*, leading to the optimal PFR of $\Omega^* = 1$.

5.4. *Air consumption*

Using (17) in combination with (25), a characteristic equation for the air consumption is derived:

$$V_n = A_k L \frac{p_s}{p_0} = \frac{\pi^2 \Omega^2}{p_0} \frac{mL^2}{T_f^2} = K_V \frac{mL^2}{T_f^2}. \tag{50}$$

It shows two interesting relations when the cylinder is dimensioned according to (25):

- The air consumption does not depend on the supply pressure level.
- The air consumption depends quadratically on the transition time.

These statements are valid for a constant PFR. Thus, a reduced supply pressure is compensated by a larger cylinder, such that the air consumption remains the same. A similar result is shown in (Krichel *et al*. 2014), where the efficiency of low-pressure networks is treated.

The second statement shows that if the transition time is required to be halved, the air consumption is quadrupled. This indicates that if the output of a machine shall be increased by a reduction of the cycle times, the resulting energy consumption increases disproportionately.

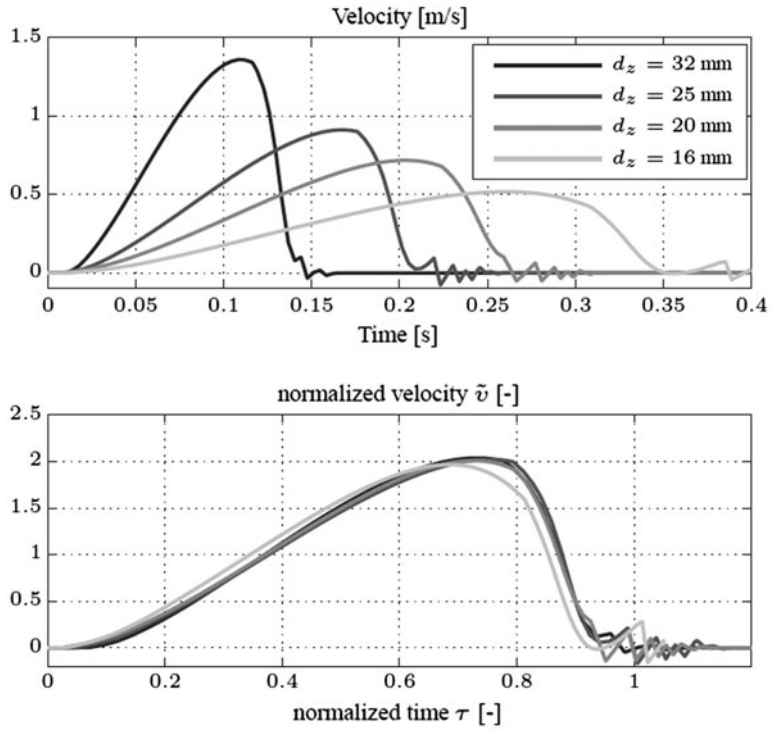

Figure 7. Similar velocity profiles for several cylinders with equal parameters: l_c = 0,1 m, m = 10 kg, p_s = 7 bar. The achieved transition times correlate to a constant PFR of Ω = 0.98.

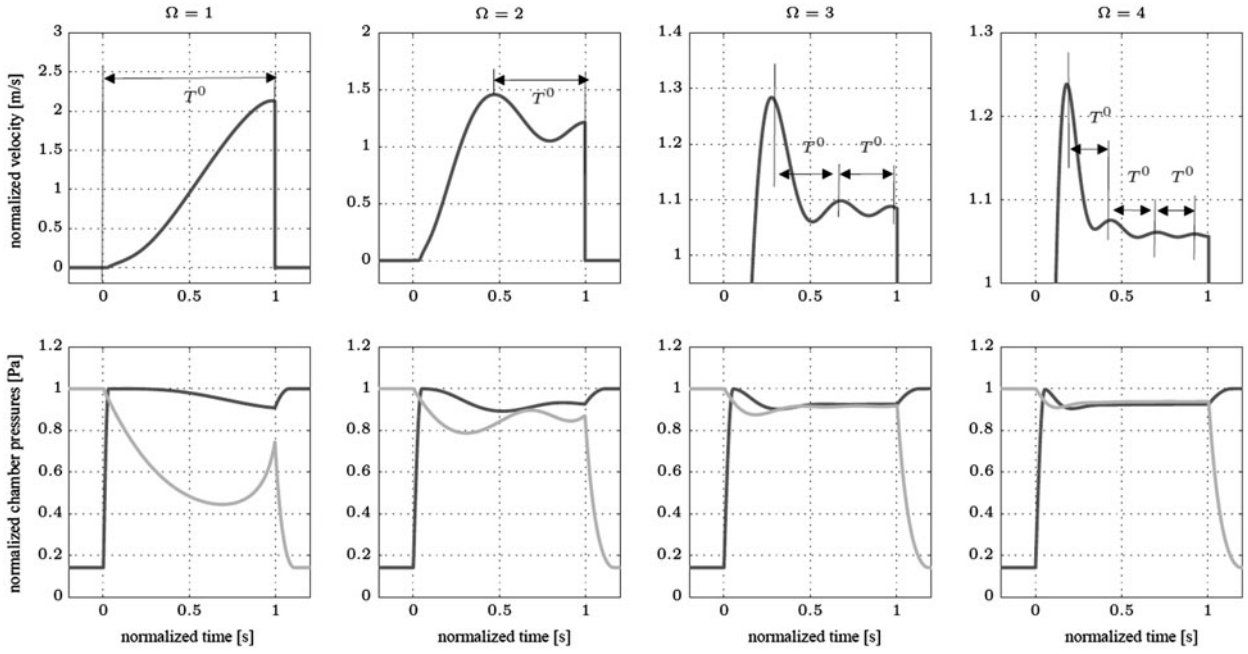

Figure 8. Comparison of the system dynamics without pneumatic cushioning by means of the velocity and the pressure profiles for integer-based PFRs: Ω = 1, 2, 3, 4. The application parameters are: m = 6 kg, l_c = 0.3 m, T_f = 0.5 s, p_s = 7 bar.

5.5. *Reduction of supply pressure*

The preceding examples show that an energy-efficient system dimensioning is achieved by using Ω = 1. This causes the systems to be reduced in diameter and eventually tiny systems for large masses are calculated. Indeed, the application can be fulfilled, but practical aspects regarding mechanical stress of the rod or the guidance conflict with the pure pneumatic dimensioning. Mechanical aspects like the workload of the bearing have to be considered in the dimensioning process but often lead to

Table 2. Classification of pneumatic cylinders in horizontal orientation by means of the PFR and a relative damping length of $l_{rel,damp} = 0.043$.

PFR Ω	Characteristics of the system dynamics
<0.9	Under-dimensioned cylinder, hardly realisable (only with hydraulic shock absorbers)
0.9…1.1	Under-dimensioned cylinder, only with hydraulic shock absorbers
1.1…1.7	Well-dimensioned cylinder, pneumatic cushioning possible
1.7…2.2	Slightly oversized cylinder, good motion dynamics with almost stationary velocity
2.2…2.5	Oversized cylinder
>2.5	Strongly oversized cylinder

oversized systems from an energetic point of view. Therefore, mechanical aspects cause additional air consumption. To compensate this, a reduction of the supply pressure level is possible. Again (23) is used for the derivation of a characteristic equation for the supply pressure level:

$$p_s = \Omega^2 \left(\frac{\pi}{T_f}\right)^2 \frac{mL}{A_k} = K_P \frac{mL}{A_k T_f^2}. \tag{51}$$

If the cylinder size is given, the calculated pressure level p_s leads directly to energy savings according to (17). Thus, energy efficiency is achieved, although an oversized cylinder is used.

Regarding the results of Section 4, a variation of the supply pressure level causes residual errors in the system dynamics, such that the system dynamics cannot be transferred exactly (see Table 2). Therefore, the supply pressure shouldn't be reduced below 3 bar (Krichel *et al.* 2014).

6. Conclusion

This paper shows a new approach for sizing pneumatic cylinders. The approach comes from similarity considerations of differently parameterised pneumatic systems. It is shown that the eigenfrequency of a pneumatic cylinder is a characteristic quantity expressing the possible speed of the system. A new characteristic factor is introduced with the PFR, which expresses the ratio between the demanded speed and the possible speed. The dimensioning approach is validated by using the differential equations of the system dynamics. It is shown that the PFR approach does not compensate all the nonlinearities; especially the friction force has an influence on residual errors. Using huge validation data, optimal values for the PFR are achieved. The PFR expresses that an energy-efficient dimensioning is achieved, if both the eigenfrequency and the frequency correlated to the transition time match, i.e. $\Omega = 1$. This is an interesting result because a lot of biological systems (as humans or animals) always make use of the eigenfrequency to save energy. With respect to pneumatic cylinders, it indicates that the piston should oscillate between both the end positions in one wave. An operation outside the eigenfrequency indicates waste of energy.

The applicability of the PFR is quite larger: It is shown that the PFR characterises the system dynamics, such that it can be used for classification purposes. It can be used to dimension systems with approximately constant speed, and it delivers interesting relations between all the system parameters. Furthermore, it can be used to increase energy efficiency by calculating a reduced, correct pressure level for existing, oversized systems.

Nomenclature

Abbreviations

CACOS	Computer Aided Cylinder Optimisation System, Simulation software of Festo AG & Co. KG
PFR	pneumatic frequency ratio Ω
PTP	point to point

Symbols

A	area [m²]
$\mathcal{A}$	application parameters
b	b value [–]
c	stiffness [N/m]
C	sonic conductance [m³ s^{-1} Pa^{-1}]
d	diameter [m]
$\boldsymbol{D}$	scaling matrix
$\dot{e}$	error dynamics
f	friction coefficient
$\boldsymbol{f}$	system function
F	force [N]
g	acceleration of gravity [m s^{-2}]
k	throttling factor [–]
K	proportional constant
l	length [m]
L	characteristic length [m]
m	load [kg]
$\dot{m}$	mass flow [kg s^{-1}]
$\dot{\tilde{m}}$	positive mass flow [kg s^{-1}]
$\dot{\bar{m}}$	mean mass flow [kg s^{-1}]
n	polytropic exponent [–]
p	pressure [Pa]
$\boldsymbol{p}$	parameter vector
q	pressure ratio [–]
R	gas constant [J kg^{-1} K^{-1}]
$\mathcal{S}$	system parameters
t	time [s]
T	temperature [K]
T^0	period at eigenfrequency [s]
T_f	transition time [s]
u	input, valve position
V	volume [m³]
W	energy/work [J]
x	position [m]
$\boldsymbol{x}$	state vector

$\tilde{\boldsymbol{x}}$	normalised state vector
α	angle of cylinder [rad]
ω	frequency [rad s^{-1}]
Ω	pneumatic frequency ratio [–]
ψ	flow function [–]
ρ	densitiy of air [kg m^{-3}]
Σ	system
τ	normalised time
ξ	ratio of areas [–]
ζ	scaling factor [–]

Note

1. CACOS has been used for over 10 years and in 2014 more than 280000 simulations have been done. CACOS is online accessible with the following link: http://www.festo.com/cat/en-gb_gb/DKI3ProPneu.asp.

Notes on contributors

Matthias Doll received his diploma degree in engineering cybernetics from the University of Stuttgart, Stuttgart, Germany, in 2009. He is currently working toward his PhD degree in a joint project with Festo AG & Co. KG, Esslingen, Germany. Since 2009, he has been a research assistant with the Institute for System Dynamics, University of Stuttgart. Since 2012, he is a research engineer at Festo AG & Co. KG, Esslingen, Germany. His main research interests include modelling and control of pneumatic drive systems, with a focus on energy efficiency.

Rüdiger Neumann received his diploma degree in mechanical engineering from the University of Paderborn, Germany and Trent Polytechnic, Nottingham, UK, in 1986, and PhD degree in robotics and control from the University of Paderborn and Ulm, Germany, in 1995. Since 1996, he has been an engineer of automation and control in the Research Department, Festo AG & Co. KG, Esslingen, Germany, where he is currently the head of the Department of Mechatronic Systems. His research interests include the control of pneumatic and electrical servo drives, as well as control of multiaxes systems and robots.

Oliver Sawodny received his diploma degree in electrical engineering from the University of Karlsruhe, Karlsruhe, Germany, in 1991, and PhD degree from the University of Ulm, Ulm, Germany, in 1996. In 2002, he became a full professor at the Technical University of Ilmenau, Ilmenau, Germany. Since 2005, he has been the director of the Institute for System Dynamics, University of Stuttgart, Stuttgart, Germany. His current research interests include methods of differential geometry, trajectory generation and applications to mechatronic systems.

References

Asco, 2005. Pneumatikzylinder, doppeltwirkend [Double-acting pneumatic cylinders]. Product sheet, ASCO, JOUCOMATIC. Available from: www.ascojoucomatic.de.

Bala, H.P., 1985. Durchflussmessungen und strömungstechnische Kenngrößen [Flow measurements and fluidic characteristic numbers]. *O+P Ölhydraulik und Pneumatik*, 29 (7), 541–544.

Bimba, 2011. *Pneumatic application & reference handbook*. Handbook. Monee, IL: Bimba Manufacturing Company.

Danks, C., 2008. The 10 most-common mistakes made when sizing pneumatic rodless actuators. *Machine design*, March, 64–67.

Dikici, A., 2004. *PX: pneumatics expert, a case-based expert system for the configuration of single-drive pneumatic systems*. Master thesis, Hochschule Esslingen.

Eschmann, R., 1994. *Modellbildung und Simulation pneumatischer Zylinderantriebe* [Modelling and simulation of pneumatic cylinders]. Dissertation. Technische Hochschule Aachen (Shaker Verlag).

Foy, M., 2003. Right-sizing pneumatic valves. *Machine design*, 75 (8), 80–82.

Göttert, M., 2003. *Bahnregelung servopneumatischer Antriebe* [Tracking control of servo pneumatic drives]. Dissertation. Universität Siegen (Shaker Verlag).

Harvey, C., 2003. Right-sizing pneumatic motion systems. *Machine design*, 75 (23), 72–80.

Hildebrandt, A., 2009. *Regelung und Auslegung servopneumatischer Aktuatorsysteme* [Control and design of servopneumatic drive systems]. Disseration. Universität Stuttgart, (Shaker Verlag), Aachen.

ISO8778, 2003. *Pneumatic fluid power – standard reference atmosphere*. 2nd ed., 2003-03-5.

Kreher, T.W., 2009. Efficient [green] pneumatic plumbing and component sizing. *Fluid power journal*, 6.

Krichel, S., Gauchel, W., and Kefer, J., 2014. Genauer hinsehen lohnt sich! Niederdruckpneumatik ist kein Garant für verbesserte Energieeffizienz [Looking closer is worth! Low pressure pneumatics does not guarantee an improved energy efficiency]. *O+P Ölhydraulik und Pneumatik*, 7–8, 20–27.

Malloy, J., 2000. 10 quick guidelines for sizing pneumatic actuators. *Power engineering*, 104 (10), 114–116.

Ohligschläger, O., 1990. *Pneumatische Zylinderantriebe – thermodynamische Grundlagen und digitale simulation* [Pneumatic cylinder drives – thermodynamic principles and digital simulation]. Dissertation. RWTH Aachen.

Sanville, F.E., 1971. A new method of specifying the flow capacity of pneumatic fluid power valves. BHRA 2nd International Fluid Power Symposium. Guildford, England, Paper D3, 37–47.

Scholz, D., 1990. *Auslegung servopneumatischer Antriebssysteme* [Design of servopneumatic drive systems]. Dissertation. RWTH Aachen.

Weiß, A., 2008. Mit Druckluft sparsam umgehen [Saving compressed air]. *Fluid spezial Drucklufttechnik*, 2, 12–14.